CrossMark

RESEARCH PAPER

Short-term variation in benthic phosphorus transfer due to discontinuous aeration/oxygenation operation

Tetsunori Inoue[1,2] · Shogo Sugahara[3] · Yasushi Seike[3] · Hiroshi Kamiya[2,4] · Yoshiyuki Nakamura[5]

Abstract The short-term dynamics of soluble reactive phosphorus (SRP) transport across the sediment surface in a brackish lake due to discontinuous aeration and oxygenation operations were investigated using laboratory and field experimental and analytical procedures. According to a laboratory incubation experiment using intact sediment cores, SRP release from the sediment was clearly suppressed by aeration, and substantial negative SRP transfer was observed during oxygenation treatment, while a positive value was observed for N_2 bubbled cores. A remarkable but impermanent increase in SRP release rate was observed within 1 or 2 days of discontinuing the aeration and oxygenation, respectively, and the release rate rapidly deceased to a quasi-steady value under N_2 bubbling conditions. An analytical model could quantitatively reproduce these laboratory experimental results for anoxic and aerated conditions, showing that this impermanent increase

was attributable to the rapid release of accumulated SRP in the oxic surface layer of the sediment. Field experiments using an in situ oxygenator showed the same tendency as the laboratory experiments, but with much larger values of the benthic SRP transfer rate. Overall, the short-term dynamics of benthic SRP transport caused by discontinuous aeration and oxygenation are considered to be an important process for the phosphorus cycle in the field.

Keywords Hypolimnetic oxygenation · Soluble reactive phosphorus release · Short-term dynamics · Eutrophic lagoon

✉ Tetsunori Inoue
  inoue-t@ipc.pari.go.jp

1 Marine Information and Tsunami Department, Port and Airport Research Institute, 3-1-1 Nagase, Yokosuka 239-0826, Japan

2 Research Center for Coastal Lagoon Environments, Shimane University, 1060 Nishikawatsu, Matsue 690-8504, Japan

3 Graduate School of Science and Engineering, Shimane University, 1060 Nishikawatsu, Matsue 690-8504, Japan

4 Shimane Prefectural Institute of Public Health and Environmental Science, 582-1 Nishihamasada, Matsue 690-0122, Japan

5 Graduate School of Urban Innovation, Yokohama National University, 79-5 Tokiwadai, Hodogaya-ku, Yokohama 240-8501, Japan

Introduction

Although phosphorus is an essential element for all organisms, excessive accumulation of this element causes eutrophication (e.g., Wang et al. 2008). As a consequence of human activity, soluble reactive phosphorus (SRP) accumulates in sediment and is released into overlying water (Fillos and Swanson 1975), acting as an internal load in various lakes and reservoirs (Gomez et al. 1999). Because benthic SRP release is substantially affected by the oxidation–reduction potential (e.g., Ahlgren et al. 2011), many operations have been applied as restoration measures supplying oxygen into deep waters to interrupt benthic SRP release (Hupfer and Lewandowski 2008). Technical approaches to supplying oxygen can be grouped into three categories: artificial destratification, hypolimnetic aeration, and hypolimnetic oxygenation.

Artificial destratification can achieve substantial reductions in oxygen depletion and heavy metal release from sediment. It is regarded as a practical approach and has been used in many lakes and reservoirs (Burns 1998; Ismail

🍪 Springer

et al. 2002; Chipofya and Matapa 2003). Well-designed hypolimnetic aerators do not cause significant destratification or warming of hypolimnetic water, but do result in measurable increases in hypolimnetic oxygen concentration and decreases in dissolved hydrogen sulfide, methane, and ammonia (McQueen and Lean 1986). Therefore, hypolimnetic aeration is also considered an effective means of supplying oxygen to the hypolimnion and suppressing benthic SRP release in stratified lakes, reservoirs, and borrow pits (Beutel and Horne 1999), and some studies have quantified its effects (Ashley 1983). However, there are a number of potential problems associated with both approaches, such as altering the thermal conditions or increasing induced oxygen demand, which affect habitat conditions for cold-water species (Beutel and Horne 1999).

Although most hypolimnetic aeration systems use air as an oxygen source (Beutel and Horne 1999), pure oxygen is more effective and has been attempted as an alternative approach (Prepas et al. 1997). One of the first successful applications of hypolimnetic oxygenation was the side stream pumping system introduced by Fast et al. (1975a). Since their study, other hypolimnetic oxygenation systems have been proposed and investigated. For example, Gantzer et al. (2009) investigated a full-scale hypolimnetic oxygenation system installed in a drinking water-supply reservoir, finding that it was able to reduce the bulk average of soluble Mn concentration in the hypolimnion by as much as 97 %. Other studies have been summarized in Beutel and Horne (1999) and Singleton and Little (2006). Advantages of hypolimnetic oxygenation systems include their high oxygen-transfer efficiency and ability to minimize turbulence introduced into the hypolimnion and induced oxygen demand, without accidental destratification (Beutel and Horne 1999) or dissolved nitrogen supersaturation (Fast et al. 1975b; Fast and Lorenzen 1976).

The effects of hypolimnetic aeration and oxygenation in the control of benthic phosphorus release have been reported (Prepas and Burke 1997). As benthic phosphorus release directly relates to the oxidation–reduction potential at the sediment surface (Boström et al. 1988; Ishikawa and Nishimura 1989; Inoue and Nakamura 2012), hypolimnetic aeration and oxygenation are expected to be the most effective approaches to reducing benthic phosphorus release. However, from a mid- to long-term standpoint, there is no clear evidence that hypolimnetic oxygenation permanently suppresses benthic phosphorus release (Katsev et al. 2006; Hupfer and Lewandowski 2008). Nevertheless, short-term phosphorus dynamics caused by fluctuations in environmental conditions should be given attention from an operational perspective.

While field observations are generally conducted at 1-week or longer intervals to reveal the mid- or long-term effects of aeration/oxygenation (e.g., Prepas and Burke

1997), benthic phosphorus release responds much more quickly to fluctuations in oxidation reduction conditions (Gächter and Meyer 1993; Inoue et al. 2000; Wang et al. 2008). This makes the interpretation of field data difficult. However, to our knowledge, few papers regarding the short-term behavior of phosphorus dynamics with regard to hypolimnetic oxygenation have been published (Löfgren and Böstrom 1989; Gunnars and Blomqvist 1997). Therefore, in the present study, the short-term dynamics of phosphorus transfer across the sediment–water interface within 1 week of starting or stopping aeration and oxygenation were investigated, using laboratory incubation experiments with intact sediment cores from a borrow pit in a brackish lake. To compensate for somewhat rough spatial and temporal resolutions in laboratory experiments, more precise examinations were conducted via a numerical diffusion model, and the results were compared with the laboratory experimental results. Moreover, benthic transfer rates of phosphorus were estimated from the results of a field experiment in which a chamber oxygenator was employed in the bottom layer of the borrow pit.

Materials and methods

Site description

Lake Nakaumi, a shallow eutrophic lagoon (86.8 km^2 in area, 5.4 m mean depth), is located at the Shimane and Tottori prefectural border in western Japan. It is connected with Lake Shinji through the Ohashi River, which flows into the southwestern side of Lake Nakaumi (Godo et al. 2001; Fig. 1). Although the lake connects to the Japan Sea via the Sakai Channel, major water exchange is driven by wind-induced current, because the ambient tide level is as small as ~ 15 cm in amplitude at the Sakai Channel mouth (Ishitobi et al. 1993). Seawater intrusions are occasionally induced by the passage of low pressure, resulting in a stagnant bottom layer with stable vertical stratification (Masuki et al. 2011). Intact sediment cores were collected from the central point (35°26'17''N, 133°16'23''E; Fig. 1) of a man-made borrow pit in the eastern part of Lake Nakaumi using Plexiglas cores. The cross-section of the borrow pit has a rectangular shape and the water depth at the central point varies from 14 to 15 m because of changes in tidal or weather conditions. Density stratification is stable in summer, and vertical temperature and salinity profiles are horizontally homogeneous in the borrow pit. On average, the salinity is 20.9 and 31.7 psu in the surface and bottom layers, respectively. Dissolved oxygen in the hypolimnion is completely depleted during summer because of the stable density stratification.
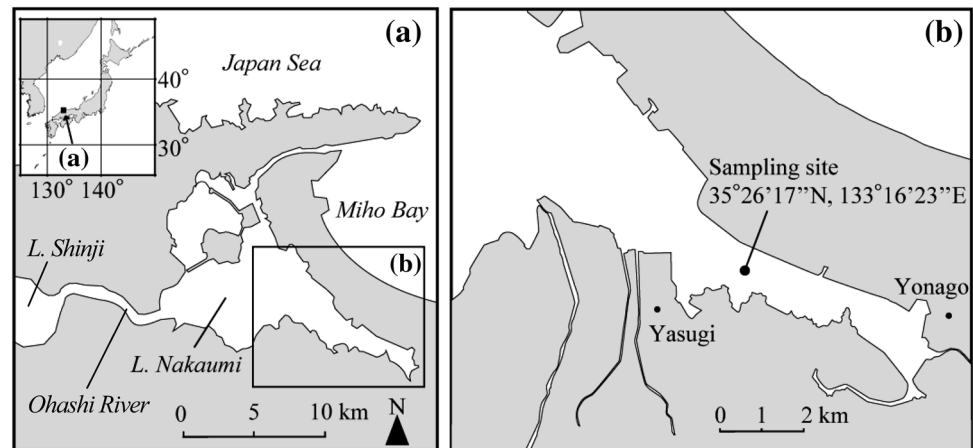
Laboratory incubation experiment

In the laboratory experiment, intact sediment cores taken from the sampling site mentioned above were incubated for 1 week, and benthic SRP release rates were estimated from the rate of temporal change in SRP concentration in the core water. In this section, the procedure employed in the laboratory incubation experiment is described in detail.

Intact sediment cores were sampled by scuba diving on 28 September 2007 under steadily anoxic conditions, using Plexiglas pipes (85 mm diameter, 500 mm height). These cores were immediately transported to the laboratory and placed in an experimental room at constant temperature to maintain the water temperature at 25 °C, nearly identical to the in situ temperature at the sampling site. To minimize the effects of biochemical reactions in the overlying water, filtered overlying water collected near the sediment cores collection site was carefully poured into the core to exchange overlying water with water containing no sediment suspension. The O_2 concentration in the overlying water was controlled by N_2, air, or O_2 bubbling during pre-incubation at an intensity sufficiently low to avoid resuspension of the sediment particles. During this process, the overlying water was well mixed. Although no measured data were available to our study regarding the thickness of the diffusive boundary layer (DBL) immediately above the sediment–water interface, it was expected to be thinner in sediment cores than in situ because of the bubbling. Therefore, the air/O_2 bubbling experiment was considered to have been conducted under effectively oxygen-supplied conditions. Triplicate cores were prepared for each condition and the experiment was done in the dark, except when the overlying water was sampled.

After 1 day of pre-incubation, which was inferred to be sufficient to achieve in situ conditions in the experimental system (e.g., Glud et al. 1999), deployment #1 was begun and continued for one day. Three experimental conditions (N_2, air, and O_2 bubbling) were established in this deployment. Overlying water was sampled using a tube with an inlet placed ∼50 mm above the sediment surface without exposure to the air, and a portion of the sampled water was immediately filtered using a disposable filter with a pore size of 0.45 μm (Minisalt SM16555 K, Saltrius, Tokyo, Japan). Filtered and nonfiltered samples were bottled separately in acid-washed polypropylene bottles and stored at −25 °C in a freezer until chemical analyses were conducted as described below. SRP release rates from the sediment were calculated based on differences in SRP concentration in the overlying water between the start and finish times of the deployment. After deployment #1 was complete, air or O_2 bubbling was changed to N_2 bubbling and deployment #2 was commenced, which continued for five days. During this period, the overlying water was sampled at 1-day intervals and SRP release rates were calculated by the slope of the concentration variation as a function of time. Oxygen concentrations in the overlying water were basically measured at the sampling times using an oxygen electrode (DO-24P, TOA DKK, Tokyo, Japan), but at ∼10-min intervals immediately after the deployment initiation.

After the laboratory incubation experiment, known volumes of particular sediment layers were quarried using end-cut syringes from some sediment cores. Portions of the quarried sediment were centrifuged at 3000 rpm for 10 min to separate pore water in N_2-filled tubes. The obtained pore water was then collected by syringe to avoid exposing it to the air, after which it was filtered using a disposable filter of pore size 0.45 μm (Minisalt SM16555 K, Saltrius, Tokyo, Japan) and stored at −25 °C in a freezer until chemical analysis. These data were used as boundary conditions and the molar ratio of SRP to ferrous iron for analytical model calculation, as described below.

The porosity, volume-specific oxygen consumption rate, and SRP adsorption/desorption rates of the sediment were also measured immediately after completion of the laboratory incubation experiment. Some known-volume

portions of the quarried sediment collected using end-cut syringes were dried at 60 °C for 2 days. Afterward, the porosity was estimated from the difference in the weights before and after drying, considering the pore water density. Other portions were used to measure the volume-specific oxygen consumption rate of the sediment, which was determined by following the method of Hosoi et al. (1992). This involved measuring the decreasing rate of O_2 concentration in bottom water of known volume (376 mL) clouded with sediment of known volume (~ 8.3 cm^3). The rate was defined as the total oxygen consumption rate. This rate was also determined for sample water spiked with formalin to suppress biological activity. This was assumed to be the chemical oxygen consumption rate (Urban-Malinga and Opalinski 1999), equal to the rate constant of ferrous iron oxidation. Moreover, differences between the total and chemical oxygen consumption rates were defined as the biological oxygen respiration rate. Volume-specific SRP adsorption and desorption rates were also measured following a procedure similar to that used to determine the volume-specific oxygen consumption rate, but with measurement of the rates of decrease and increase of the SRP concentration in the water, respectively. Specifically, wet sediment of known volume (~ 6.3 cm^3) was suspended in bottom water of known volume (550 mL) that had been bubbled with N_2 gas beforehand, and the rate at which the SRP concentration (initially 1.4 µmol L^{-1}) increased was monitored to obtain the SRP desorption rates. For SRP adsorption rates, almost the same procedure was followed, but air-bubbled and SRP-added bottom water (initial concentration 1112.5 µmol L^{-1}) was used. These parameters were utilized in the subsequent analyses (Table 1).

Because the pH was not measured in the experiment described above, we conducted an additional experiment to investigate pH changes related to N_2 bubbling. Intact sediment cores were sampled by the same procedure at the same sampling site, and were incubated for 5 days with N_2 bubbling. pH in the overlying water was measured twice daily during the additional experiment using a pH electrode (Multi 340i, WTW, Weilheim, Germany).

Field oxygenator experiment

A field experiment to investigate hypolimnetic oxygenation was conducted at the aforementioned sampling site, using the water environmental preservation (WEP) system (Matsue Doken Co., Ltd., Matsue, Japan), in 2009. The WEP system is a submerged contact chamber oxygenator that has a submergible pump capable of discharging 120–150 m^3 h^{-1} of water through a duct of radius 0.2 m, attached to the bottom of a chamber of radius 1.4 m and height 3.2 m (Masuki et al. 2011). As the WEP system dissolves oxygen gas instead of air in discharge water, the oxygen concentration in that water reaches a high level. This concentration depends on the water depth at which the system is installed, with values of 1560 and 2190 µmol L^{-1} at depths of 10 and 20 m, respectively (Yajima and Masuki 2009).

In our study, the WEP system was suspended from a floating vessel to a depth of 13.8 m at the sampling site, and it was operational was from 16 April to 1 October 2009. Vertical profiles of water temperature, salinity, and oxygen concentration were observed intermittently using a multi-data sonde (DS-5X, Hydrolab, Loveland, CO, USA) during system operation and a few weeks before and after operation. At the same time, water was sampled to obtain the vertical profile of the SRP concentration. Measurement and sampling were also conducted in an adjacent area within 300 m of the experimental site.

Chemical analysis

Ammonium, nitrite, nitrate, and SRP of filtered water and pore water samples were analyzed by the indophenol, colorimetric, cadmium reduction-colorimetric, and ascorbic acid methods (Clesceri et al. 1998) using a

Table 1 Parameters used to estimate benthic SRP release in the study

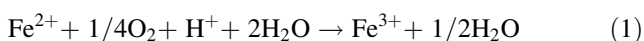| Parameter	Notation	Value	Unit
Apparent diffusion coefficient of O_2	D_{zO}	2.29×10^{-3}	mm^2 s^{-1}
Apparent diffusion coefficient of SRP	D_{zP}	4.60×10^{-4}	mm^2 s^{-1}
Apparent diffusion coefficient of ferrous iron	D_{zF}	4.60×10^{-4}	mm^2 s^{-1}
Porosity	ϕ	0.96	–
Rate constant of ferrous iron oxidation	k_{OF}	1.71×10^6	mm^3 mmol^{-1} s^{-1}
Rate constant of oxygen respiration	k_B	5.00×10^{-11}	s^{-1}
Rate constant of SRP adsorption	k_{ad}	6.62×10^{-4}	s^{-1}
Rate constant of SRP desorption	k_{de}	1.56×10^{-5}	s^{-1}
Molar ratio of SRP to ferrous iron	α	84.2	–

D_{zO} is cited from Boudreau (1996), and D_{zP} and D_{zF} are cited from Ishikawa and Nishimura (1989). Other parameters were obtained from experimental results described in this paper

spectrophotometer (TRAACS800, Bran + Luebbe, Norderstedt, Germany). Total nitrogen and phosphorus concentrations of filtered and nonfiltered water and pore water samples were analyzed by the cadmium reduction-colorimetric and ascorbic acid methods, respectively, after persulfate digestion (SWAAT, BL TEC K.K., Tokyo, Japan). Particulate nitrogen and phosphorus concentrations were calculated by subtracting the dissolved total nitrogen and phosphorus concentrations from the total nitrogen and phosphorus concentrations, respectively.

Values of total iron content in the water and sediment were measured by atomic absorption photometry (Z-5000, Hitachi High-Technologies Co., Tokyo, Japan) after decomposition using persulfate potassium solution for 50 min. Values from the filtered pore water were equated with ferrous iron concentrations.

Analytical model assessment of the sediment–water interface

Generally, phosphorus in sediment is considered to exist as authigenic minerals, organic materials, and to be adsorbed on sediment particles (Sasaki et al. 2001). Since iron redox changes are most frequently found to be responsible for short-term sediment–phosphorus sorption or desorption (Gunnars and Blomqvist 1997; Gonsiorczyk et al. 2001), oxygen, SRP, and ferrous iron were formulated following Inoue et al. (2000). The model used herein considers the dynamics of ferric hydroxide-bound SRP separately and consists of a diffusion model for the DBL and a transport/reaction model for the sediment. In this model, O_2 is supplied by diffusion from the overlying water to the sediment, after which it is consumed by biological oxygen consumption (i.e., respiration) and chemical oxygen consumption (i.e., oxidation of ferrous iron in the sediment). Basically, SRP in the pore water is supplied by solid materials, for example through desorption from sediment particles, dissolution of ferrous phosphate, and others. In addition, owing to the oxidation–reduction potential, SRP is adsorbed on ferric hydroxide under oxic conditions, and is supplied by desorption from ferric hydroxide under anoxic conditions. The processes considered herein—oxidation of ferrous iron, SRP supply from solid materials, and SRP adsorption to and desorption from ferric hydroxide—were expressed as follows:

$$Fe^{2+} + 1/4O_2 + H^+ + 2H_2O \rightarrow Fe^{3+} + 1/2H_2O \quad (1)$$

$$PO_4^{3-} \leftarrow PO_4^{3-}(solid) \quad (2)$$

$$mFeOOH + nPO_4^{3-} \rightleftarrows (FeOOH)_m \equiv (PO_4^{3-})_n, \quad (3)$$

where m and n are numerical coefficients showing the composition ratio of SRP adsorption to ferric hydroxide. In

this study, we did not formulate the pH variations caused by any of the diagenetic reactions stated above because buffer action in the pore water was considered to dominate. SRP supply from the decomposition of organic matter was not formulated either, because it was considered negligible for short-term phenomena. This is discussed later.

Following Ishikawa and Nishimura (1989), let us assume that an equilibrium of SRP exchange between pore water and the solid phase is established in the bulk region of the sediment. For the surface region of the sediment, the net supply of SRP was formulated to be proportional to the difference between the SRP concentrations there and in the bulk region. Consequently, the mass balance equations were formulated as follows:

$$\phi \frac{\partial C_O}{\partial t} = \phi D_{zO} \frac{\partial^2 C_O}{\partial z^2} - \frac{1}{4}\phi k_{OF} C_O C_F - k_B C_O, \quad (4)$$

$$\phi \frac{\partial C_P}{\partial t} = \begin{cases} \phi D_{zP} \frac{\partial^2 C_P}{\partial z^2} - k_{ad} C_P - k_{de}\{C_P - C_P(-\infty)\} & (C_O > 0) \\ \phi D_{zP} \frac{\partial^2 C_P}{\partial z^2} + k_{de} P_P - k_{de}\{C_P - C_P(-\infty)\} & (C_O = 0) \end{cases}, \quad (5)$$

$$\frac{\partial P_P}{\partial t} = \begin{cases} +k_{ad} C_P & (C_O > 0) \\ -k_{de} P_P & (C_O = 0) \end{cases}, \quad (6)$$

$$\phi \frac{\partial C_F}{\partial t} = \phi D_{zF} \frac{\partial^2 C_F}{\partial z^2} - \phi k_{OF} C_O C_F - \frac{1}{\alpha} k_{de}\{C_P - C_P(-\infty)\}, \quad (7)$$

where C_O, C_P, and C_F are the concentrations of O_2, SRP, and ferrous iron in pore water, respectively, P_P is the SRP adsorbed on ferric hydroxide (values were converted to the equivalent concentration in the pore water for convenience), D_{zO}, D_{zP}, and D_{zF} are the apparent diffusion coefficients of O_2, SRP, and ferrous iron, respectively, in the sediment (Boudreau 1996), t is time, z is the vertical axis from the sediment–water interface (positive upward and zero at the sediment–water interface), ϕ is the porosity, k_{OF} is the rate constant of ferrous iron oxidation, k_B is the rate constant of respiration, k_{ad} is the rate constant of SRP adsorption on ferric hydroxide, k_{de} is the rate constant of SRP desorption from ferric hydroxide and supply from solid materials, α is the molar ratio of increments of SRP and ferrous iron concentrations, and $C_P(-\infty)$ is the SRP concentration in pore water at $z = -\infty$.

Here, k_{OF} and k_B are assumed to be identical to the chemical and biological oxygen consumption rates stated in the previous section, respectively (Ishikawa and Nishimura 1989). The second terms on the right-hand side of Eq. 5 show the SRP adsorption on or desorption from ferric hydroxide produced by the oxygen supply. These terms were simply formulated as functions of SRP concentration

without considering the ferric hydroxide concentration, because we could not find any certain relationship between the SRP adsorption or desorption rates and ferric hydroxide concentration in the laboratory experiment. The third terms on the right-hand sides of Eqs. 5 and 7 show the basic supplies of SRP from solid materials. Actually, the SRP and ferrous iron balances were affected by processes such as SRP desorption from sediment particles, FeS formation, and others. Here, we simply used the measured molar ratio of SRP to ferrous iron in the pore water at depths of 40–60 mm as α, considered to be the overall supply ratio. For simplicity, nitrate and manganese were not formulated because their presence was not relevant to the main conclusions of this work. Bioturbation and bioirrigation were not considered because no macro- or meiobenthos were found in the laboratory experiment.

The analytical calculation followed the procedure described below. As a pre-calculation, stable solutions for vertical profiles of the respective components were calculated under anoxic conditions. These were considered in situ profiles and were used as initial conditions for the main calculations. Three independent calculations simulating pre-incubation and deployment #1 were conducted in which 0, 215, and 938 $\mu mol\ L^{-1}$ were given as upper boundary conditions for O_2, respectively. Next, the vertical profiles obtained from the aforementioned calculations were given as initial conditions for the subsequent calculations to simulate deployment #2, with the O_2 upper boundary being 0 $\mu mol\ L^{-1}$. The parameters used are summarized in Table 1.

Results

Laboratory experimental results

SRP was the dominant fraction of phosphorus in the overlying water, accounting for ~96.7 % of the total phosphorus on average throughout the experiment. Ammonium was the dominant fraction of nitrogen, representing ~66.7 % of the total nitrogen and ~99.8 % of the dissolved inorganic nitrogen on average. Because little nitrite and nitrate was detected and their values were <0.6 $\mu mol\ L^{-1}$ even under O_2 bubbling conditions, they were not responsible for the oxidation–reduction potential and SRP release in the sediment cores.

Deployment #1 was conducted for 1 day (Fig. 2). During this deployment, oxygen concentrations in the overlying water were kept at 0 $\mu mol\ L^{-1}$ for N_2 bubbling conditions, ~215 $\mu mol\ L^{-1}$ for air bubbling, and 938 $\mu mol\ L^{-1}$ for O_2 bubbling, respectively. We found a large positive value (0.43 ± 0.09 mmol m^{-2} day^{-1}) that was within a reasonable range previously reported (Sinke
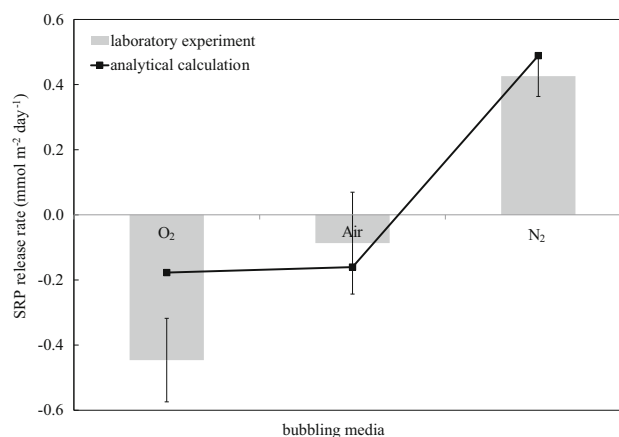

Fig. 2 Laboratory experimental results for SRP release rates under O_2, air, and N_2 bubbling conditions (i.e., during deployment #1). Negative values show SRP transfer from water to sediment. *Columns* are laboratory experimental results from deployment #1, and *squares* are corresponding results from analytical calculations. *Error bars* are standard deviations

et al. 1990) for N_2 bubbled cores. However, SRP release for air-bubbled cores was obviously suppressed (−0.09 ± 0.16 mmol m^{-2} day^{-1}). Moreover, values observed under O_2 bubbling were strongly negative (−0.45 ± 0.13 mmol m^{-2} day^{-1}), indicating substantial SRP transfer from overlying water to the sediment. The differences among the calculated SRP release rates of the three bubbling media were clearly significant.

After deployment #2 commenced, the oxygen concentration in the overlying water rapidly fell to 0 $\mu mol\ L^{-1}$ within an hour. The time series of SRP release rates for cores continuously bubbled with N_2 gas was stable but gradually decreased (from 0.43 ± 0.09 to 0.23 ± 0.04 mmol m^{-2} day^{-1}) with time during the deployment (Fig. 3). This was likely because of a gradual weakening of the SRP concentration gradient at the sediment–water interface, which was caused by an increase in SRP concentration in the overlying water (see the next section). Conversely, the other two treatments showed remarkably positive maximum SRP release rates on the first day for ex-air-bubbled cores (1.66 ± 0.24 mmol m^{-2} day^{-1}, calculated from the increase in SRP concentration between $t = 0$ and 1 days of deployment #2) and second day for ex-O_2-bubbled cores (1.82 ± 0.16 mmol m^{-2} day^{-1}, calculated from the increase in SRP concentration between $t = 1$ and 2 days of deployment #2). Both of these marked increases were temporary, and values decreased continuously for the next few days, finally reaching almost the same values (0.40 ± 0.01 mmol m^{-2} day^{-1} for ex-air-bubbled cores and 0.33 ± 0.08 mmol m^{-2} day^{-1} for ex-O_2-bubbled cores) as the cores continuously bubbled with N_2.

SRP and ferrous iron concentrations in the filtered pore water obtained from depths of 40–60 mm were 193.6 and
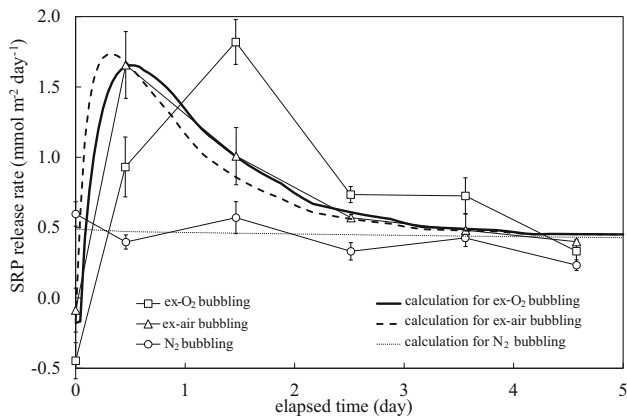
Fig. 3 Laboratory experimental results for the time series of SRP release rates from sediment after N_2 bubbling commenced (i.e., during deployment #2). *Squares*, *triangles*, and *circles* are laboratory experimental results from ex-O_2-, ex-air-, and ex-N_2-bubbled cores, respectively, and *error bars* are standard deviations. *Thick solid*, *dashed*, and *thin dotted lines* correspond to results of analytical calculations of ex-O_2-, ex-air-, and ex-N_2-bubbled cores, respectively. Values from deployment #1 are also plotted, at $t = 0$

2.3 µmol L^{-1}, respectively, resulting in $\alpha = 84.2$ (Table 1). This value was used in the analytical calculation described below. The results from the additional experiment concerning pH variation showed a slight and continuous increase of pH in the overlying water, from 8.33 to 8.56 over 94.8 h. We do not believe that this increase was critical, as per the discussion regarding its effects on SRP release given below.

Analytical calculation results

This section reports analytical results from the numerical model, which consists of a diffusion model of the DBL and a transport/reaction model of the sediment. The parameters used in this study are summarized in Table 1. Here, α was simply calculated from SRP and ferrous iron concentrations in pore water. Since substantial ferrous iron must combine with sulfide, α was larger than previously reported (Gunnars and Blomqvist 1997). That is, α represents multiple parameters such as SRP desorption and iron-sulfide production.

The calculated SRP release rates of 0.49 mmol m^{-2}-day^{-1} for N_2-bubbled cores and -0.16 mmol m^{-2} day^{-1} for air-bubbled cores in deployment #1 were quantitatively in good agreement with the experimental results (Fig. 2), but the analytically calculated SRP scavenging rate for O_2 bubbling treatment (-0.18 mmol m^{-2} day^{-1}) underestimated the large negative value obtained from experimental cores (-0.45 ± 0.13 mmol m^{-2} day^{-1}).

The calculated vertical O_2 profiles at the end of deployment #1 showed that the O_2 penetration depth was 2.6 mm for air bubbling and 7.2 mm for O_2 bubbling

(Fig. 4a). The difference in calculated penetration depth was simply a result of the difference in O_2 concentration at the upper boundary (i.e., the bulk region of overlying water). Because a brown-colored layer was confirmed at the sediment surface in deployment #1 of the laboratory incubation experiment, these analytical results were qualitatively consistent with the experimental results, showing evidence for the oxidation of ferrous iron. The SRP concentration decreased substantially in the oxic layer after the air and O_2 bubbling because of adsorption on ferric hydroxide (Fig. 4b), and the layer thickness reflected the respective O_2 profiles. Hydroxide-bound SRP (P_P) in the oxic layer showed similar maximum values in both the air and O_2 bubbling treatments, but the range of the layer reflected the respective oxic layer thickness (Fig. 4c). Both profiles showed two peaks at the edges of the oxic layer. The upper and lower peaks reflected an accumulation of SRP transported by diffusion from the water column and the deeper part of the sediment, respectively.

Such hydroxide-bound SRP accumulation in a specific surface layer caused rapid SRP release after terminating air and O_2 bubbling in deployment #2 (Fig. 3). The calculated variation in this release for ex-air-bubbled cores satisfactorily reproduced the experimental result, although that for ex-O_2 bubbling failed to reproduce the time lag prior to reaching the maximum release value. The calculated SRP release rate under N_2 bubbling showed a slight and gradual decrease simply because of the increase in SRP concentration at the upper boundary (i.e., in the overlying water). This was qualitatively consistent with the experimental result, but the model result underestimated the rate of decrease. The gradual decrease observed in the experiment may have been in part because of the decrease in SRP supply from sediment particles.

Field experimental results

During WEP operation, the salinity in the surface and bottom layers was 8–10 and 30–33 psu, respectively. A steep vertical gradient of salinity was observed at a depth of around 5 m, which persisted throughout the period. Total iron was not detected in the overlying water before and during the experiment. Before starting the operation, the oxygen concentration in the hypolimnion was ~ 9 µmol L^{-1}. After the operation commenced, the oxygenated water mass was confirmed to be distributed within a 70-m radius in the horizontal and a 3-m thickness in the vertical, while the oxygen concentration in the mass remained ~ 313 µmol L^{-1}. After oxygenation was stopped, the concentration in the hypolimnion decreased to ~ 6 µmol L^{-1}.

The SRP concentration in the overlying water decreased considerably 4 days after the start of oxygenation, from 6.1

Fig. 4a–c Analytically calculated vertical profiles of **a** O$_2$, **b** SRP, and **c** hydroxide-bound SRP (P_P). *Thick, normal,* and *thin lines* are analytical results for ex-O$_2$-, ex-air-, and ex-N$_2$-bubbled cores, respectively. P_P values were converted to the equivalent concentration in the pore water. *Zero on the vertical axis* represents the sediment–water interface. Figure 4b provides a schematic explanation of λ, originally defined by Ishikawa and Nishimura (1989) from calculations of the SRP concentration gradient at the sediment–water interface and the SRP concentration in the bulk region
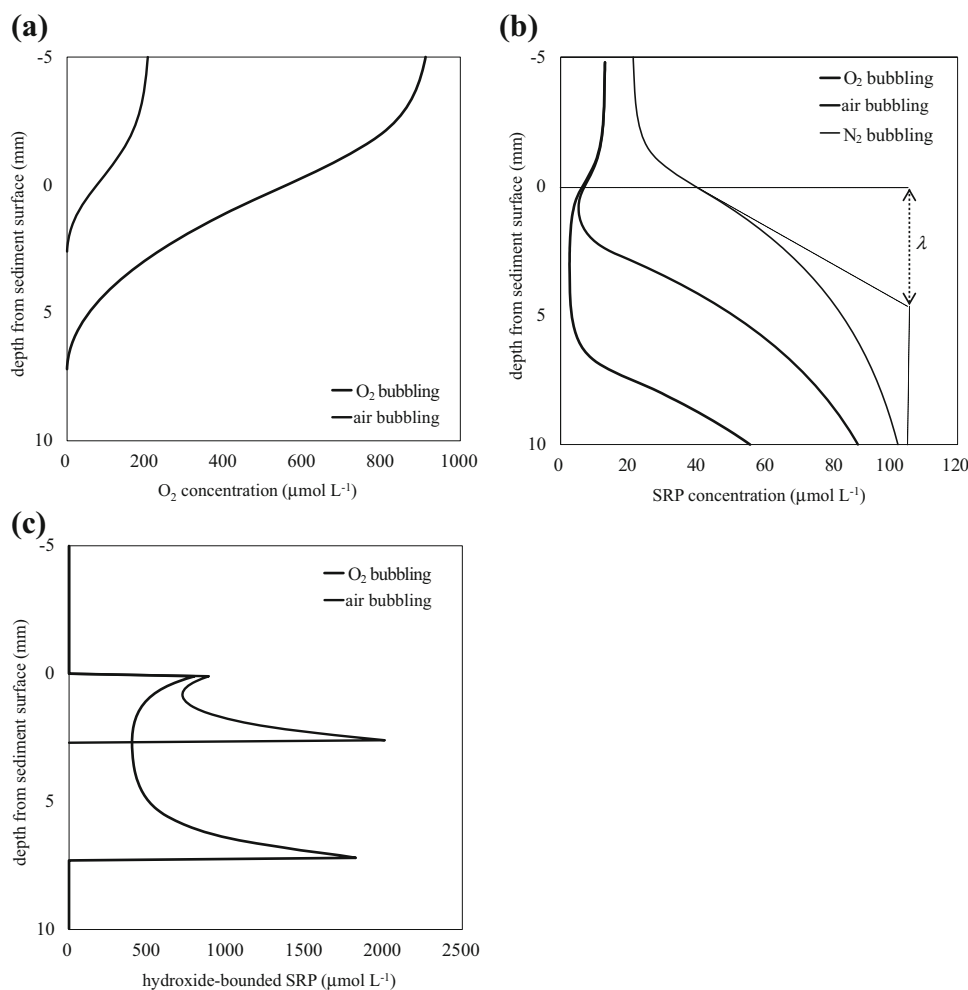
to 3.1 µmol L^{-1} at 15 m and 3.6 to 2.3 µmol L^{-1} at 13 m (Fig. 5a). Because the density stratification was stable and there was no obvious current in the borrow pit (Masuki et al. 2011), it was assumed that this decrease was caused by the sedimentation of oxidized materials adsorbing SRP and/or direct SRP adsorption on the oxidized sediment surface. Based on these results, the average area-specific SRP rate of decrease was calculated at −1.43 mmol m^{-2} day^{-1} for the 4-day period, revealing a 44 % decrease in SRP concentration in the bottom layer.

The SRP concentration in the overlying water increased considerably after oxygenation was stopped, from 7.5 to 26.1 µmol L^{-1} at 15 m and 7.5 to 18.0 µmol L^{-1} at 13 m (Fig. 5b). During this period, the density stratification stabilized, with no obvious current in the borrow pit (Masuki et al. 2011). This increase was considered attributable to the release of SRP that had been adsorbed on the oxidized sediment surface. Based on these results, the area-specific SRP increase (i.e., release) rate was calculated at 10.33 mmol m^{-2} day^{-1} on average for the 4-day period. This rapid release caused the SRP concentration in the

bottom layer to increase threefold. Both of the short-term phenomena above were important and exerted effects on the hypolimnetic environment in the borrow pit.

Discussion

Omitted processes in analytical model assessment

In this study, the SRP supply from the decomposition of organic matter was not formulated. Thus, let us make a tentative calculation to evaluate the SRP supply rate associated with the aerobic decomposition of organic matter. Assuming the oxygen concentration in the pore water to be 100 µmol L^{-1}, the respiration rate k_B-$C_O = 5.00 \times 10^{-9}$ µmol L^{-1} s^{-1}. Moreover, assuming that the composition ratio of phosphorus to carbon of organic matter is 1/106, the SRP supply rate is calculated as 3.62×10^{-11} µmol L^{-1} s^{-1}, based on the molar ratio of O$_2$ respiration to SRP supply. This value shows that the SRP supply from aerobic decomposition for seven days is
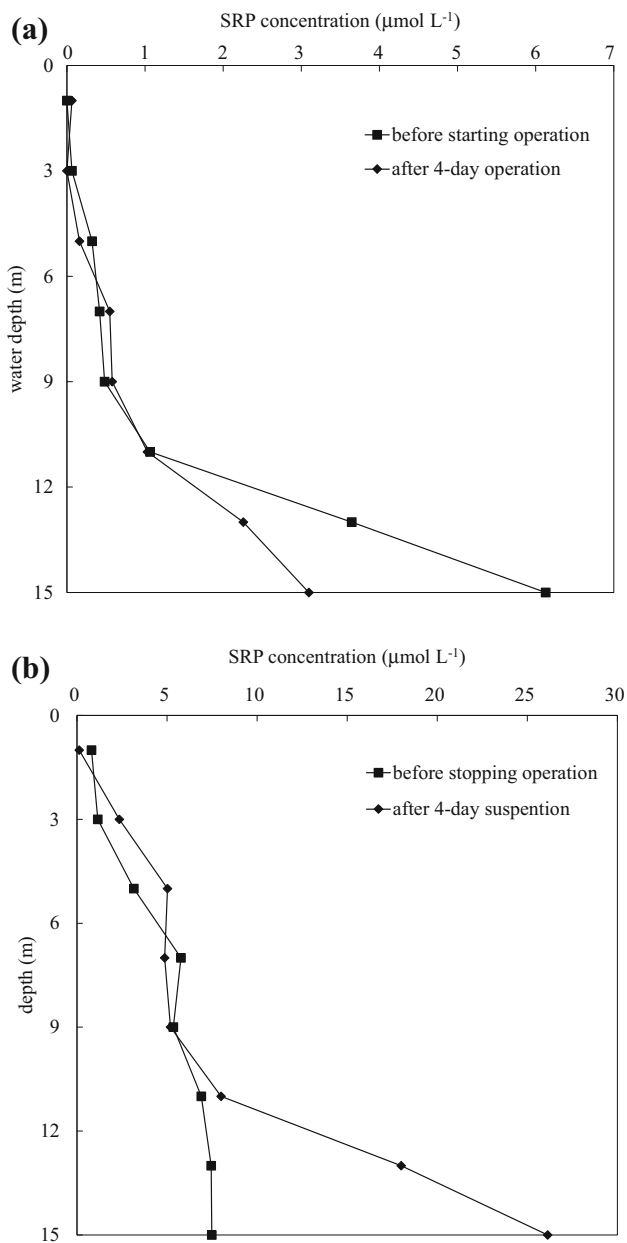
Fig. 5a–b Observed vertical profile of SRP concentration at the field experimental site. **a** Before (*squares*) and after (*diamonds*) starting oxygenation; **b** before (*squares*) and after (*diamonds*) oxygenation termination

2.19×10^{-5} µmol L^{-1}, which is much smaller than the SRP concentration in the pore water. Therefore, in this study, it was reasonable not to formulate the SRP supply from the decomposition of organic matter.

Additionally, some diagenetic processes cause hydrogen/hydrogen carbonate ion production or consumption and may alter the sediment pH profile. Because in our previous study (Nakamura et al. 1996) a certain pH change in the oxic layer was not confirmed and the pH decrease in the anoxic layer was considered to be induced by organic acid accumulation,

we did not formulate pH dynamics in the present study. However, other research works (e.g., Nielsen et al. 2010) have shown a slight pH change in the surface layer, so pH may be a candidate component in the additional formulation. Further studies are required to address the pH variation caused by certain diagenetic processes in detail.

Bacterial SRP accumulation and release

Gächter et al. (1988) conducted laboratory experiments with cultures of bacteria in the surface sediment to identify conditions under which sedimentary microorganisms might contribute to phosphorus uptake and release. They showed that bacteria in the surface sediment grown in aerobic media released substantial SRP after the cultures became anoxic, and that the release occurred over more than 60 h. In our experiment, a remarkable increase in SRP release rates was observed within 48 h, after which they decreased continuously for the next few days. Consequently, the timescales of the SRP release variations were considerably different from each other. Moreover, the duration of air or O_2 bubbling was only 48 h, which was considered insufficient for the establishment of a stable phase of an aerobic bacterial community, and aerobic or facultative anaerobic bacterial accumulation and release of SRP (Fleischer 1983) were considered to be minor. Therefore, we inferred that the temporal increases in SRP release rates after conditions became anoxic were not caused by the release from bacteria but rather by desorption from ferric hydroxide, as shown in the calculated results (Fig. 3).

However, Fleischer (1986) stated that the microorganism-mediated phosphorus uptake process occurs before or coincides with chemical adsorption. Because we do not have any data describing the aerobic or facultative anaerobic bacterial density, and because their phosphorus uptake increased during air or O_2 bubbling, further studies are required to quantify the contribution of temporal biotic processes to total benthic phosphorus release after a shift from aerobic to anaerobic conditions.

Effect of pH increase on SRP release

The additional experiment showed that N_2 bubbling induced a slight and continuous increase of pH in the overlying water, from 8.33 to 8.56 over 94.8 h. The pH change was probably caused by interactions between the CO_2 decrease and other buffering processes. Lijklema (1980) experimentally studied the adsorption isotherms of SRP on ferric hydroxide, and obtained their ratio as a function of pH and ambient SRP concentration as follows:

$$\frac{P_P}{P_{Fe}} = 0.298 - 0.0316\text{pH} + 0.201C_P^{1/2}, \tag{8}$$

where P_{Fe} is the ferric hydroxide content and C_P is in mmol L^{-1}. Assuming that a representative C_P value is 0.01 mmol L^{-1}, P_P/P_{Fe} should be 0.0549 at pH 8.33 and 0.0476 at pH 8.56. This possibly shows that the pH change caused by N_2 bubbling induces a 13 % decrease in SRP adsorption potential. Based on the P_P content profile shown in Fig. 4c, a 13 % desorption of P_P over the entire sediment range for 94.8 h increases the SRP released by 0.09 mmol m^{-2} day^{-1} in the air-bubbled case and 0.15 mmol m^{-2} day^{-1} in the O$_2$-bubbled case. These values are small versus the transfer rate shown in Figs. 2 and 3.

The increase of pH in the sediment was considered to be restricted to the immediate vicinity of the surface and did not affect the adsorption ratio in the deeper part of the sediment. In addition, the observed pH increase was weak and did not cause the remarkable temporal increase after N$_2$ bubbling commenced. Moreover, Patrick and Khalid (1974) stated that pH has little effect on the oxidation state of the iron compounds under anaerobic conditions. Based on these considerations, we concluded that the effect of the change in pH from the CO$_2$ decrease caused by N$_2$ bubbling had no effect on the overall conclusions of our study.

Negative SRP transport

The laboratory and field experiments revealed a substantial decrease in SRP concentration in the overlying water during air or O$_2$ bubbling. Possible explanations for these findings are (1) SRP coprecipitation with any materials (Dittrich et al. 1997), (2) diffusive transport of SRP from the water to the sediment, or a combination of these two processes.

According to Ashley (1983), hypolimnetic aeration causes coprecipitation of major ions (e.g., Ca^{2+}, Mg^{2+}) and phosphorus accompanied by an increase in turbidity. In our laboratory incubation experiment, no increase in turbidity in the overlying water was observed, and the particulate phosphorus concentration remained at a much smaller value than the SRP. Moreover, total iron was not detectable in the overlying water under anoxic conditions. Together, these findings imply that SRP coprecipitation with any oxidized ions made almost no contribution to the decrease in SRP concentration during air or O$_2$ bubbling.

The formation of ferric hydroxide, which adsorbs SRP, is generally considered one of the major sink terms of SRP in pore water (Mortimer 1971). Because the model prediction reproduced this reasonably well, the negative SRP release shown in the air/O$_2$-bubbled cores was considered to be diffusive transport caused by the decrease of SRP concentration at the oxic sediment surface. However, the analytically calculated SRP scavenging rate for O$_2$

bubbling treatment underestimated the large negative value obtained from laboratory experimental cores. This finding implies that oxygenation might have effects other than oxidation of ferrous iron. Possible other processes, such as oxidation of manganese (Gonsiorczyk et al. 1998) or changes in the physiology of sediment bacteria caused by fluctuations in oxidation–reduction conditions (Pomeroy et al. 1965; Prepas and Burke 1997), should also be determined to explain the faster transport shown in O$_2$-bubbled cores.

Both laboratory and field experimental data showed the same qualitative tendency for SRP transfer from the overlying water to sediment after the start of oxygenation. However, those transfer rates differed greatly from each other. The average field value of SRP transfer from oxygenation was calculated at -1.43 mmol m^{-2} day^{-1} for the 4-day period, three times larger than the laboratory experimental value (-0.45 mmol m^{-2} day^{-1}). In the laboratory experiment, the amount of SRP in the overlying water was limited and SRP transfer was likely near completion within a day. This probably explains the smaller laboratory experimental value relative to the field value.

Temporary increase in SRP release rate after oxygenation is halted

Oxygenation creates an increased mobile phosphorus pool at the sediment surface that may be released when oxygenation is halted (Liboriussen et al. 2009). Our results show that this phenomenon is important and occurs within a few days of suspending oxygenation.

In the present study, SRP desorption and diffusion in the sediment were considered to be the controlling processes for the temporary increase in SRP release after discontinuing air or O$_2$ bubbling. The timescale for SRP desorption, τ_{de}, and that for SRP diffusion in the sediment, τ_s, are defined as follows (Inoue et al. 2000):

$$\tau_{de} = \frac{1}{k_{de}}, \qquad (9)$$

$$\tau_s = \frac{\lambda^2}{2D_{zP}}, \qquad (10)$$

where λ is the length scale of the vertical SRP concentration profile in the sediment. λ was originally defined by Ishikawa and Nishimura (1989) and was calculated from the SRP concentration gradient at the sediment–water interface and the SRP concentration in the bulk region (schematically shown in Fig. 4b).

In our study, we used 1.56×10^{-5} s^{-1} for k_{de}, which resulted in $\tau_{de} = 17.8$ h. We assumed that λ was expressed as the length scale of oxic layer formed by bubbling, because it strongly affects the fluctuation in SRP release

rate immediately after discontinuance of bubbling. Since λ values were 2.6 mm for air bubbling and 7.2 mm for O_2 bubbling, τ_s values were calculated at 2.2 h for ex-air bubbling and 16.8 h for ex-O_2 bubbling. Calculated time lag of SRP release in response to the discontinuance of bubbling were expressed well by applying combinations of these phenomena (Fig. 3). This finding shows the importance of frequent field observations, especially after environmental alterations.

However, the model prediction failed to reproduce the same time lag of SRP release as seen in the ex-O_2-bubbling system of the SRP release experiment. The difference in time lag between the experiment and analytical calculation was ~ 1 day. This failure might have occurred because the numerical model did not formulate the oxidation–reduction potential and did not reproduce its decrease at the sediment surface after oxygenation was discontinued. Therefore, the SRP desorption started immediately after O_2 depletion in the model analysis, even though it took about 2 days to reach the maximum release value in the laboratory incubation experiment.

Implications for oxygenation operations

In our laboratory incubation experiment, total SRP releases from ex-air (average 4.12 mmol m^{-2}) and ex-O_2 (average 4.54 mmol m^{-2}) bubbled cores during the 5-day incubation of deployment #2 were more than twice those from ex-N_2 bubbled cores (average 1.96 mmol m^{-2}), in accord with the results reported by Hupfer and Lewandowski ([2008]). Because the initial SRP concentration in the overlying water before pre-incubation was 19.3 µmol L^{-1}, the amount of SRP adsorption on the sediment surface was estimated at 1.50 ± 0.44 mmol m^{-2} for air-bubbled cores and 2.11 ± 0.40 mmol m^{-2} for O_2-bubbled cores during pre-incubation and deployment #1. These values explained the difference in total SRP releases between the ex-air/O_2 bubbled cores and ex-N_2 bubbled cores reasonably well.

Although it is difficult to address quantitatively, the field experiment also showed the same increasing tendency in SRP release rate (10.33 mmol m^{-2} day^{-1}) after oxygenation termination. This was probably caused by a sudden release of accumulated SRP at the sediment surface. Cowell et al. ([1987]) also reported that SRP concentrations increased markedly after aeration equipment malfunctions, and the annual mean release was significantly greater than mean values for aeration and pre-aeration years. This might have been caused by a sudden release of accumulated phosphorus at the sediment surface during hypolimnetic aeration suspension. These findings indicate that oxygenation operations should not be suspended under anoxic conditions, and that suspending operations for only a few days will cause a sudden release of adsorbed phosphorus, offsetting the results of the previous long-term operation.

Conclusions

In the present study, the short-term dynamics of SRP transport across the sediment surface caused by discontinuous aeration/oxygenation were investigated by experimental and analytical methods. Laboratory incubation experiments were conducted under radical conditions, with pure oxygen used as a bubbling medium and the maximum O_2 concentration reaching 900 µmol L^{-1}. However, even under such radical conditions, the effects of oxygenation did not persist for more than 2 days, and suppressed SRP was released over the next few days. Field experiments showed the same tendencies as the laboratory experiments but much larger values of SRP release. This difference was probably caused by the much larger in situ SRP content than that in the laboratory. Thus, even if oxygenation affects the transitory binding of phosphorus at the sediment surface, it does not continue binding after the operation is discontinued. Taken together, these results indicate that hypolimnetic aeration and oxygenation are only temporarily effective approaches to suppressing benthic SRP release. The effects will not be maintained without aeration/oxygenation operations, and there will be a dramatic release of the phosphorus accumulated at the sediment surface during hypolimnetic aeration and oxygenation within a few days of discontinuing operations.

SRP dynamics respond to fluctuations in environmental conditions more quickly than other components, which means that spatially and temporally local phenomena have substantial effects on the phosphorus balance at the sediment–water interface. Such local variations in benthic phosphorus release may make it difficult to interpret field data regarding aeration/oxygenation. Given this characteristic, more detailed and frequent observations will be required to enable a quantitative understanding of the phosphorus cycle in the field. Moreover, a quantitative understanding of short-term processes will aid more efficient operation of the in situ aerator and oxygenator, e.g., temporary oxygenation from a forecast of seawater intrusion or strong winds and temporary suspension of oxygenation during a stable period, among others.

References

Ahlgren J, Reitzel K, De Brabandere H, Gogoll A, Rydin E (2011) Release of organic P forms from lake sediments. Water Res 45:565–572

Ashley KI (1983) Hypolimnetic aeration of a naturally eutrophic lake: physical and chemical effects. Can J Fish Aquat Sci 40:1343–1359

Beutel MW, Horne AJ (1999) A review of the effects of hypolimnetic oxygenation on lake and reservoir water quality. Lake Reservoir Manag 15:285–297

Boström B, Andersen JM, Fleischer S, Jansson M (1988) Exchange of phosphorus across the sediment–water interface. Hydrobiologia 170:229–244

Boudreau BP (1996) Diagenetic models and their implementation. Springer, New York

Burns FL (1998) Case study: automatic reservoir aeration to control manganese in raw water Maryborough town water supply Queensland, Australia. Water Sci Technol 37:301–308

Chipofya VH, Matapa EJ (2003) Destratification of an impounding reservoir using compressed air—case of Mudi reservoir, Blantyre, Malawi. Phys Chem Earth Pt A/B/C 28:1161–1164

Clesceri LS, Greenberg AE, Eaton AD (1998) Standard methods for the examination of water and wastewater. APHA/AWWA/WEF, Washington, DC

Cowell BC, Dawes CJ, Gardiner WE, Scheda SM (1987) The influence of whole lake aeration on the limnology of a hypereutrophic lake in central Florida. Hydrobiologia 148:3–24

Dittrich M, Dittrich T, Sieber I, Koschel R (1997) A balance analysis of phosphorus elimination by artificial calcite precipitation in a stratified hardwater lake. Water Res 31:237–248

Fast AW, Lorenzen MW (1976) Synoptic survey of hypolimnetic aeration. J Env Eng Div–ASCE 102:1161–1173

Fast AW, Dorr VA, Rosen RJ (1975a) A submerged hypolimnion aerator. Water Resour Res 11:287–293

Fast AW, Overholtz WJ, Tubb RA (1975b) Hypolimnetic oxygenation using liquid oxygen. Water Resour Res 11:294–299

Fillos J, Swanson WR (1975) The release rate of nutrients from river and lake sediments. J Water Poll Control Fed 47:1032–1041

Fleischer S (1983) Microbial phosphorus release during enhanced glycolysis. Naturwissenschaften 70:415

Fleischer S (1986) Aerobic uptake of Fe(III)-precipitated phosphorus by microorganisms. Arch Hydobiol 107:269–277

Gächter R, Meyer JS (1993) The role of microorganisms in mobilization and fixation of phosphorus in sediments. Hydrobiologia 253:103–121

Gächter R, Meyer JS, Mares A (1988) Contribution of bacteria to release and fixation of phosphorus in lake sediments. Limnol Oceanogr 33:1542–1558

Gantzer PA, Bryant LD, Little JC (2009) Controlling soluble iron and manganese in a water-supply reservoir using hypolimnetic oxygenation. Water Res 43:1285–1294

Glud RN, Gundersen JK, Holby O (1999) Benthic in situ respiration in the upwelling area off central Chile. Mar Ecol Prog Ser 186:9–18

Godo T, Kato K, Kamiya H, Ishitobi Y (2001) Observation of wind-induced two-layer dynamics in Lake Nakaumi, a coastal lagoon in Japan. Limnol 2:137–143

Gomez E, Durillon C, Rofes G, Picot B (1999) Phosphate adsorption and release from sediments of brackish lagoons: pH, O_2 and loading influence. Water Res 33:2437–2447

Gonsiorczyk T, Casper P, Koschel R (1998) Phosphorus-binding forms in the sediment of an oligotophic and an eutrophic hardwater lake of the Baltic Lake district (Germany). Water Sci Technol 37:51–58

Gonsiorczyk T, Casper P, Koschel R (2001) Mechanisms of phosphorus release from the bottom sediment of the oligotrophic Lake Stechlin: importance of the permanently oxic sediment surface. Arch Hydobiol 151:203–219

Gunnars A, Blomqvist S (1997) Phosphate exchange across the sediment–water interface when shifting from anoxic to oxic conditions—an experimental comparison of freshwater and brackish–marine systems. Biogeochemistry 37:203–226

Hosoi Y, Murakami H, Kozuki Y (1992) Oxygen consumption by bottom sediment. Proc JSCE Hydraul Sanit Eng 456/II:83–92 **(in Japanese)**

Hupfer M, Lewandowski J (2008) Oxygen controls the phosphorus release from lake sediments—a long-lasting paradigm in limnology. Int Rev Hydrobiol 93:415–432

Inoue T, Nakamura Y (2012) Response of benthic soluble reactive phosphorus transfer rates to step changes in flow velocity. J Soils Sediments 12:1559–1567

Inoue T, Nakamura Y, Adachi Y (2000) Non-steady variations of SOD and phosphate release rate due to changes in the quality of the overlying water. Water Sci Technol 42:265–272

Ishikawa M, Nishimura H (1989) Mathematical model of phosphate release rate from sediments considering the effect of dissolved oxygen in overlying water. Water Res 23:351–359

Ishitobi Y, Kamiya H, Itogawa H (1993) Tidal, meteorological and hydrological effects on the water level variation in a lagoon, Lake Shinji. Jpn J Limnol 54:66–79

Ismail R, Kassim MA, Inman M, Baharim NH, Azman S (2002) Removal of iron and manganese by artificial destratification in a tropical climate (Upper Layang Reservoir, Malaysia). Water Sci Technol 46:179–183

Katsev S, Tsandev I, L'Heureux I, Rancourt DG (2006) Factors controlling long-term phosphorus efflux from lake sediments: exploratory reactive-transport modeling. Chem Geol 234:127–147

Liboriussen L, Søndergaard M, Jeppesen E, Thorsgaard I, Grünfeld S, Jakobsen TS, Hansen K (2009) Effects of hypolimnetic oxygenation on water quality: results from five Danish lakes. Hydrobiologia 625:157–172

Lijklema L (1980) Interaction of orthophosphate with iron(III) and aluminum hydroxides. Environ Sci Technol 14:537–541

Löfgren S, Böstrom B (1989) Interstitial water concentrations of phosphorus, iron and manganese in a shallow, eutrophic Swedish lake—implications for phosphorus cycling. Water Res 23:1115–1125

Masuki S, Yajima H, Seike Y (2011) Injection of highly oxygenated water into the bottom of dredged area in Lake Nakaumi. Annu J Hydraul Eng JSCE 55:1525–1530 **(in Japanese)**

McQueen DJ, Lean DRS (1986) Hypolimnetic aeration: an overview. Water Pollut Res J Can 21:205–217

Mortimer CH (1971) Chemical exchanges between sediments and water in the Great Lakes—speculations on probable regulatory mechanisms. Limnol Oceanogr 16:387–404

Nakamura Y, Inoue T, Kerciku F, Sayama M (1996) Study on microstructure of diffusive boundary layer using oxygen microelectrode. Proc Coast Eng 43:1081–1085 **(in Japanese)**

Nielsen LP, Risgaard-Petersen N, Fossing H, Christensen PB, Sayama M (2010) Electric currents couple spatially separated biogeochemical processes in marine sediment. Nature 463:1071–1074

Patrick WH, Khalid RA (1974) Phosphate release and sorption by soils and sediments: effect of aerobic and anaerobic conditions. Science 186:53–55

Pomeroy LR, Smith EE, Grant CM (1965) The exchange of phosphate between estuarine water and sediments. Limnol Oceanogr 10:167–172

Prepas EE, Burke JM (1997) Effects of hypolimnetic oxygenation on water quality in Amisk Lake, Alberta, a deep, eutrophic lake with high internal phosphorus loading rates. Can J Fish Aquat Sci 54:2111–2120

Prepas EE, Field KM, Murphy TP, Johnson WL, Burke JM, Tonn WM (1997) Introduction to the Amisk Lake project: oxygenation of a deep, eutrophic lake. Can J Fish Aquat Sci 54:2105–2110

Sasaki K, Noriki S, Tsunogai S (2001) Vertical distributions of interstitial phosphate and fluoride in anoxic sediment: insight into the formation of an authigenic fluoro-phosphorus compound. Geochem J 35:295–306

Singleton VL, Little JC (2006) Designing hypolimnetic aeration and oxygenation systems—a review. Environ Sci Technol 40:7512–7520

Sinke AJC, Cornelese AA, Keizer P, Van Tongeren OFR, Cappenberg TE (1990) Mineralization, pore water chemistry and phosphorus release from peaty sediments in the eutrophic Loosdrecht Lakes, The Netherlands. Freshw Biol 23:587–599

Urban-Malinga B, Opalinski KW (1999) Vertical zonation of the total, biotic and abiotic oxygen consumption on a Baltic sandy beach. Oceanol Stud 28:85–96

Wang S, Jin X, Bu Q, Jiao L, Wu F (2008) Effects of dissolved oxygen supply level on phosphorus release from lake sediments. Colloid Surf A 316:245–252

Yajima H, Masuki S (2009) Flow mechanism generated by the hypolimnetic oxygenator WEP system in a reservoir. Annu J Hydraul Eng JSCE 53:1339–1344 **(in Japanese)**